
CHALMERS
UNIVERSITY OF TECHNOLOGY

# A Multivariate Local Rational Modeling Approach for Detection of Structural Changes in Test Vehicles

Available online at www.sciencedirect.com

ScienceDirect

IFAC PapersOnline CONFERENCE PAPER ARCHIVE

IFAC PapersOnLine 54-7 (2021) 79–84

# A Multivariate Local Rational Modeling Approach for Detection of Structural Changes in Test Vehicles ⋆

**T. McKelvey** * **D. McKelvey** ** **P. Nordberg** **

* *Chalmers University of Technology, SE-412 96 Göteborg, Sweden (e-mail: tomas.mckelvey@chalmers.se).*

** *Volvo Cars, SE-405 31 Göteborg, Sweden (e-mail: {daniel.mckelvey,patrik.nordberg}@volvocars.com).*

**Abstract:** A data driven structural change detection method is described and evaluated where the data are acceleration and force measurements from a mechanical structure in the form of a vehicle. By grouping the measured signals as inputs and outputs an hypothesized MIMO linear dynamic relation between the inputs and outputs is assumed. It is assumed that baseline data are available to build statistical models for the estimated frequency function of the baseline system at selected frequencies. When new data is available, the monitoring algorithm re-estimates the non-parametric frequency function and uses a test statistic based on the statistical distance to detect possible change. To generate the frequency function estimates a non-parametric MIMO frequency function estimator based on the local rational model (LRM) method is developed. A statistical analysis of the proposed test statistic shows that it has an F-distribution for data from the baseline case. The method is evaluated on simulated data from a high fidelity full scale vehicle simulation generating both baseline data and data from a structurally changed vehicle. In the evaluation, the frequency response functions were estimated by the non-parametric LRM method, the parametric ARX estimate and the non-parametric ETFE. The results show that all three methods can detect the structural change while the LRM method is more robust with respect to the selection of the hyperparameters.



*Keywords:* Nonparametric methods, Frequency domain identification, Statistical data analysis, Statistical methods/signal analysis for FDI, Condition Monitoring

## 1. INTRODUCTION

Autonomous drive functionality for vehicles is currently being developed at a high pace in the vehicle industry. This development also has implications on the development and test processes employed for developing new vehicles. To ensure a high degree of safety and durability of the developed products, a significant amount of various vehicle testing is part of the development chain. One such activity is durability test where the vehicles are driven on designated test tracks with road surface conditions of varying character. The high degree of autonomy available today can be used to replace the test driver in test vehicles which undergo extensive durability tests on a test track. This is for example advantageous from a cost perspective since, for the more severe tests, the test driver can only be active a limited time due to occupational health restriction on acceptable accumulated vibration levels. For safety reasons for other vehicles on the testing grounds, it is paramount that the autonomous vehicle automatically can detect serious structural changes and stop the vehicle to prevent possible accidents with other test track users. A human driver can often detect such developments early on by sensing changed vibration behavior or changes in the acoustic profile of the vehicle.

Detection of changes in a system based on signal measurements is a vast topic with many application areas and solution methods. In principle the problem boils down to generate some test statistic which discriminate between the baseline situation and the changed situation. Depending on the application domain, knowledge in terms of intermediate models can be useful to find good test statistics. In the book Basseville and Nikiforov (1993) a good overview of applications can be found and a comprehensive description of methods and analysis based on a statistical setting. The old overview paper Doebling et al. (1996) give a comprehensive list of approaches for structural monitoring techniques which focus on detecting changes in frequencies of flexible modes or in mode shapes. Yin et al. (2014) gives an overview of monitoring methods based on various statistical tools as PLS and PCA. An approach to structural damage detection based on estimation of transmissibility is outline in Johnson and Adams (2002) which uses a global modeling setting in order to locate the damaged structure. A global modeling approach for structural monitoring is given in Basseville et al. (2004) where a stochastic subspace-based covariance-driven identification method is used to design a detection algorithm. In Kopsaftopoulos and Fassois (2010) a set of parametric

⋆ This work has been performed within FFI project ETAVEP with support from Vinnova and Volvo Cars.


10.1016/j.ifacol.2021.08.338

time domain ARX model are estimated for different faults which then are used to provide residuals in a test phase to discriminate the different faults.

### 1.1 Problem formulation

The overall problem formulation is to design a system which, based on measured sensor signals, can deliver a numerical value which is measure of how different the present system is as compared to a baseline situation. The measured data are organized into input signals which provide excitation to the mechanical structure and output signals which are measurements of the resulting vibrational response. For sample index $t$ the inputs are denoted by the vector $u(t) \in \mathbb{R}^m$ and the outputs are denoted by the vector $y(t) \in \mathbb{R}^p$ and we hypothesize that they are related by

$$y(t) = G(z)u(t) + v(t) \tag{1}$$

where $v(t) \in \mathbb{R}^p$ represent a noise signal uncorrelated with the input signal and $G(z)$ is a multi-input-multi-output (MIMO) linear system operator of size $p \times m$.

### 1.2 Overview of the solution

In this contribution we propose a structural integrity monitoring system which, based on acceleration measurements from sensors on the vehicle structure, monitor the structural response and give an estimate of a potential deviation from a baseline response. The baseline response is obtained during test drives on the track when the vehicle is guaranteed to be structurally fully functional. Our solution is based on monitoring the frequency function response from forces to accelerations at a discrete set of frequencies. To estimate the frequency function of the hypothesized linear operator in (1), we employ a multivariate extension to the local rational model (LRM) method McKelvey and Guerin (2012) which provides a non-parametric estimate of the matrix valued frequency function at arbitrary frequencies. This is in contrast with the majority of methods which use a parametric finite order model to capture the full frequency response estimate. The LRM method has a computational low complexity, is non-parametric and hence does not require difficult model order choices and does not suffer from the large variance issue spectral estimation techniques suffer from when the data window is relatively short. From the baseline data, we build a multidimensional statistical model assuming the frequency function estimates at discrete frequencies have a complex Gaussian distribution Kay (1993). In the monitoring phase the frequency functions are continuously re-estimated and the statistical distance to the baseline model is determined. This distance metric will hence provide a measure of the structural integrity of the vehicle and can be used to provide early warning to degradation or flag for severe problems which should lead to emergency stop of the vehicle to prevent further damage.

In Section 2 we derive the MIMO extension to the LRM method and formulate the statistical model for the change detection algorithm including the test statistic. In Section 3 it is described how the developed method is evaluated on experimental data generated from a high fidelity vehicle model and the results from the evaluation is presented and discussed. The distribution of the test statistic is derived in the Appendix.

## 2. METHODS

In this section we will describe the MIMO LRM method to obtain a non-parametric estimate of a MIMO frequency function based on a window of operational data comprising input and output samples. Afterwards follows a description on how the change detection procedure is designed and a discussion on the properties of the suggested test statistic.

### 2.1 MIMO local rational model (MIMO-LRM)

The LRM method for scalar valued frequency functions was introduced by McKelvey and Guerin (2012) and here we will extend the method for the MIMO frequency function case. A MIMO version of the original LRM method has also been described by Voorhoeve et al. (2018) where a matrix fraction description parametrization is introduced. The $N$-point discrete Fourier transform (DFT) of a signal $x(t)$ is defined as

$$X(k) \triangleq \sum_{t=0}^{N-1} x(t)e^{-j2\pi kt/N} \tag{2}$$

for $k = 0, 1, \ldots, N-1$. The DFT forms the basic analysis method to derive non-parametric estimates of the frequency function based on a finite window of samples of the input and output signal of the system under study.

Any causal discrete time linear system of finite McMillan degree $n$ can be described by (see e.g Kailath (1980)) a state space model of order $n$

$$\begin{aligned} x(t+1) &= Ax(t) + Bu(t) \\ y(t) &= Cx(t) + Du(t) + v(t) \end{aligned} \tag{3}$$

where $x(t) \in \mathbb{R}^n$ is the state-vector and $(A, B, C, D)$ are the state-space matrices. The system has the corresponding frequency response function

$$G(\omega) = D + C(e^{j\omega}I - A)^{-1}B \tag{4}$$

It was shown in McKelvey (2000) that the $N$-point DFT of the input and output signals are related as, for $k = 0, \ldots, N-1$

$$Y(k) = G(\omega_k)U(k) + T(\omega_k) + V(k) \tag{5}$$

where $\omega_k = 2\pi k/N$ and

$$\begin{aligned} G(\omega) &= D + C(e^{j\omega}I - A)^{-1}B \\ T(\omega) &= C(e^{j\omega}I - A)^{-1}(x(0) - x(N))e^{j\omega} \end{aligned} \tag{6}$$

This result shows that the DFT of the output $Y(k)$ is, beside the noise $V(k)$, the sum of the effect of the input, $G(\omega_k)U(k)$, and a second term $T(\omega_k)$ which depend on the initial and final state value. We also note that both $G(\omega)$ and $T(\omega)$ share the same dynamics, since the $A$ matrix is common for both of them.

The MIMO LRM method forms an estimate at frequency $\omega_k = 2\pi k/N$ by a locally parametrized model which is based on the structure in (5). Without loss of generality we can model the frequency function for each output channel individually and we parametrize the local models of $G(\omega)$ and $T(\omega)$ for frequency $k$ and output $i$ as

$$G^i_{k+r} = \frac{N^i_{k+r}}{D^i_{k+r}}, \quad T^i_{k+r} = \frac{M^i_{k+r}}{D^i_{k+r}} \tag{7}$$

where $r$ is an integer representing the distance to the center frequency $k$ and

$$\begin{aligned} N^i_{k+r} &= \sum_{s=0}^{n_{\rm LRM}} N^i_s(k) r^s \\ D^i_{k+r} &= 1 + \sum_{s=1}^{n_{\rm LRM}} d^i_s(k) r^s \\ M^i_{k+r} &= \sum_{s=0}^{n_{\rm LRM}} m^i_s(k) r^s \end{aligned} \tag{8}$$

were $d^i_s(k)$ and $m^i_s(k)$ are complex scalars and the row vector $N^i_s(k) \in \mathbb{C}^{1\times m}$ form the parameters of the model and $n_{\rm LRM}$ is the local model order. From (5) we can now express a local model for the output channel $i$ as

$$[Y(k+r)]_i = \frac{N^i_{k+r}}{D^i_{k+r}} U(k+r) + \frac{M^i_{k+r}}{D^i_{k+r}} + [V(k+r)]_i \tag{9}$$

where the notation $[\cdot]_i$ denote vector element $i$. Let $\theta^i_k$ denote a vector comprising all the local rational model parameters $\{N^i_s(k)\}_{s=0}^{n_{\rm LRM}}$, $\{d^i_s(k)\}_{s=1}^{n_{\rm LRM}}$ and $\{m^i_s(k)\}_{s=0}^{n_{\rm LRM}}$. It is clear from (9) that the model parameters appears nonlinear in the expression for $[Y(k+r)]_i$. However if both sides of (9) is multiplied by $D^i_{k+r}$ all parameters will appear linear in the equation. To estimate the parameters of the local model, DFT data at indices $k+r$ where $r = -N_w, \ldots, N_w$ ($N_w$ is the local window size) are used to form the least-squares problem

$$\begin{aligned} \hat\theta^i_k = \arg\min_{\theta^i_k} \sum_{r=-N_w}^{N_w} \big| &[Y(k+r)]_i D^i_{k+r} \\ &- N^i_{k+r} U(k+r) - M^i_{k+r} \big|^2 \end{aligned} \tag{10}$$

where $\hat\theta^i_k$ is the optimal parameter vector for output $i$ at frequency index $k$. When forming (10) some indices $k+r$ might fall outside the set $\{0, 1, \ldots, N-1\}$. In this case we use the $N-$periodic property of the DFT that for any integer $k$, it holds that $U(k+N) = U(k)$ and $Y(k+N) = Y(k)$. The MIMO LRM estimate of row $i$ in $G(\omega_k)$ then follows as

$$[\hat G_{\rm LRM}(\omega_k)]_{i,:} = \hat G^i_{k+0} = \frac{\hat N^i_{k+0}}{\hat D^i_{k+0}} = \hat N^i_{k+0} \tag{11}$$

where $[\cdot]_{i,:}$ denote row $i$ in the matrix. The number of parameters in the local model is $(n_{\rm LRM}+1)(m+1)+n_{\rm LRM}$ and a necessary conditions for the optimization problem (10) to have a unique solution is that

$$2N_w + 1 \geq (n_{\rm LRM}+1)(m+1) + n_{\rm LRM}. \tag{12}$$

### *2.2 Change detection*

To create a statistical baseline model of the system we assume the availability of $N_B$ windows of measurement data, each with $N$ samples. For each data window we estimate the value of the frequency function, i.e. the frequency function of the linear system $G$ in (1) for a given set of $Q$ frequencies $\mathcal{Q} = \{\omega_q\}_{q=1}^Q$. The values in the set can be arbitrary but is normally a subset of the DFT frequencies where the frequency function modeling is a valid approximation. The obtained frequency function estimate from data window $l$ of the frequency function $G(\omega)$ at frequency $\omega_q$ is denoted by $\hat G_{q,l} \in \mathbb{C}^{p\times m}$. These samples we assume to be drawn from a complex Gaussian distribution Kay (1993) with mean value $\operatorname{vec} G_q \in \mathbb{C}^{pm}$ and covariance $R_q \in \mathbb{R}^{pm\times pm}$, i.e.

$$\operatorname{vec} \hat G_{q,l} \sim \mathcal{CN}(\operatorname{vec} G_q, R_q) \tag{13}$$

where vec is the vectorization operator. The statistical model will hence capture the variability of the frequency function estimates when estimated from different data windows. Besides describing the variability due to noise in the measurements, the Gaussian model will also capture the variability of the the frequency function estimate which is due to the dependence on the input signal caused by possible nonlinear effects. Such effects which will increase the variance of the stochastic model.

Furthermore, we assume the estimates of the individual channels of the frequency function are uncorrelated and hence $R_q$ is a positive definite diagonal matrix and we also assume estimates for different frequencies are also uncorrelated. Based on samples from the $N_B$ analyzed data windows, the parameters of a *baseline* model is estimated by forming the standard sample estimates of the mean value and the variance of the complex Gaussian distribution viz

$$\begin{aligned} \operatorname{vec} \hat G_q &= \frac{1}{N_B} \sum_{l=1}^{N_B} \operatorname{vec} \hat G_{q,l} \\ [\hat R_q]_{i,i} &= \frac{1}{N_B - 1} \sum_{l=1}^{N_B} |[\operatorname{vec} \hat G_{q,l} - \operatorname{vec} \hat G_q]_i|^2 \end{aligned} \tag{14}$$

where $[\cdot]_{i,i}$ denote diagonal element $i$ in the matrix and $i = 1, \ldots, pm$.

For a new window of data we can form the frequency function estimate $\tilde G_q$ and generate the test statistic

$$T = c \sum_{q=1}^{Q} (\operatorname{vec} \tilde G_q - \operatorname{vec} \hat G_q)^* \hat R_q^{-1} (\operatorname{vec} \tilde G_q - \operatorname{vec} \hat G_q) \tag{15}$$

where $c$ is a scalar constant and $(\cdot)^*$ denote the complex conjugation and transpose. In Appendix A it is shown that $T$ has an $F$-distribution under the baseline conditions and the required value of $c$ for this to be true. The value of the test statistic $T$ can be used to take a decision whether a change has occurred or not. We can formalize this as hypothesis testing where we decide *no change* if $T \leq \eta$ and *change* if $T > \eta$. The detector will give a false-alarm if $T > \eta$ although the system has not changed. For a given value of the threshold $\eta$, the probability of a false alarm is given by $1 - \mathrm{CDF}(\eta)$ where CDF is the cumulative distribution function of the $F$-distribution. The probability to correctly detect a true change is highly dependent on how much the frequency function changes, i.e. how much the mean value of the complex Gaussian distribution is shifted due to the change. If we assume $\Delta G_q$ represent the shift of the mean value from the baseline case then the test statistic $T$ has a mean value shift

$$c \sum_{q=1}^{Q} \operatorname{vec}(\Delta G_q)^* \hat R_q^{-1} \operatorname{vec}(\Delta G_q) \tag{16}$$

Under the change scenario the test statistic will, if $N_B \to \infty$, converge to a random variable which is proportional to a random variable with a non-central chi-square distribution.

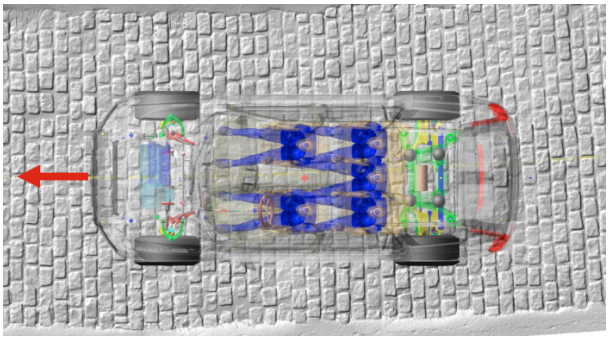

Fig. 1. Image from the simulation. The red arrow indicates the direction of movement.

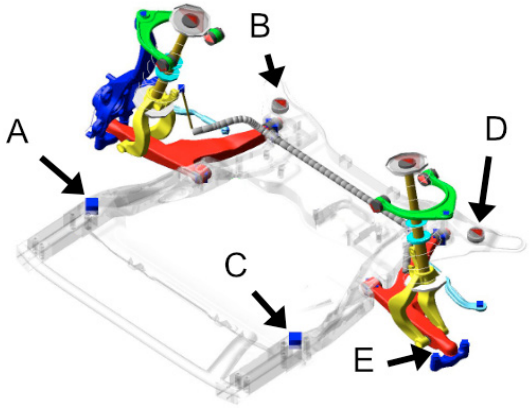


Fig. 2. Output points on sub-frame marked by A-D. Loose knuckle joint at point E.

## 3. EXPERIMENTAL EVALUATION

To evaluate the properties of the described methodology we generate data from a simulation model with high fidelity and evaluate the results.

### *3.1 Description of experiment*

The vehicle simulation model used in the experiments was developed by Volvo Cars and is a state-of-the-art multi-body system, with 2000 degrees of freedom and generates signals with a sampling rate of 1kHz. The simulation used a model of the Volvo XC90, complete with bushings, springs, dampers, etc. The road surface used in the simulations is a 3D-scan of a section of Belgian pavé at the Hällered proving ground in Sweden. See Figure 1 for a image of the model and the road surface.

Six symmetrically placed points are chosen in the front of the vehicle. For each point, accelerations in the vehicle's longitudinal and lateral direction are extracted from the model. The location of the four points on the front sub-frame is indicated by the arrows A-D in Figure 2. They represent points where accelerometers can be mounted. The two front wheel centers are taken as input points, since the road surface conditions are impractical to measure and use. Therefore we have $m = 4$ input signals and $p = 8$ output signals that represent a possible instrumentation of a real test vehicle.

The changed model has a loose ball-joint on the front-left suspension knuckle indicated by arrow E in Figure 2. The loosened joint is modeled as a bushing element with a bi-linear translational stiffness and without any rotational stiffness. The first linear translational rate is set very low to model the free stroke with a smooth transition to the normal ball joint stiffness

Four data sets, each with a length of 42 s and moving over the Belgian pavé surface were generated. For the baseline scenario, three data sets are established: when the vehicle is traveling at 36 km/h, 40 km/h and 44 km/h respectively. In addition, one data set is established for the changed model in which the vehicle has a speed of 40 km/h. We use the data sets from the 36 km/h and 44 km/h as training data to established the statistical model for the baseline. The baseline data set at 40 km/h and the 40 km/h data set for the changed model are used as test sets to validate the detection performance. The training data is split into non-overlapping data windows of size $N = 1024$ ($\sim$1s). This results in 41 data windows in each training set. This choice of data window size is motivated by a trade off between the delay to detection and and an acceptable false alarm level. The two test sets are split into windows of the same size as above, but are overlapping with an overlap of 503 data points, which results in 82 test windows. See Table 1 for an overview. The detection performance is measured by the *AUC* measure calculated from the test data. *AUC* is the area under the receiver operating characteristics (ROC) curve where $AUC = 100\%$ corresponds to a detector with no missed detections and no false alarms, see e.g. Hastie et al. (2009).

Table 1. Structure of the training and two testing sets.

| Simulation | Train | Test |
|---|---|---|
| Baseline at 36 km/h | 0–42 s | – |
| Baseline at 44 km/h | 0–42 s | – |
| Baseline at 40 km/h | – | 0–42 s |
| Loose-joint E at 40 km/h | – | 0–42 s |
| Number of windows per simulation | 41 | 82 |

### *3.2 Frequency function estimators*

For a given data window of size $N$ the frequency function is estimated at the selected frequencies in the set $\mathcal{Q}$. Here we use $N = 1024$ and $\mathcal{Q} = \{\omega_q = \frac{2\pi 4q}{N}\}_{q=1}^{Q}$ with $Q = 25$. This corresponds to 25 frequencies equally spaced between 3.9 and 97.6 Hz. In the selected frequency range the simulation model is judged to have high fidelity.

For the LRM method outlined in Section 2.1 we evaluate the method for different choices of the local window size $N_w$ and the local model order $n$.

To compare the performance of the proposed LRM frequency function estimation as part of the detector, two other frequency function estimation methods where also evaluated, a smoothed empirical frequency function estimate (ETFE) and the parametric auto-regressive with exogenous inputs (ARX) technique, see , Ljung (1999). In the ETFE method the single input single output (SISO) frequency function for each pair of input and output signals is estimated by spectral analysis

$$[\hat{G}_{\mathrm{ETFE}}(\omega_q)]_{i,j} = \frac{\hat{\Phi}_{y_i,u_j}(\omega_q)}{\hat{\Phi}_{u_j,u_j}(\omega_q)} \tag{17}$$

where $\hat{\Phi}_{y,u}(\omega_q)$ is the estimated cross-spectral density of between signals $y$ and $u$ and $\hat{\Phi}_{u,u}(\omega_q)$ is the estimated spectral density of the signal $u$. Here we use Welsh method and use local window sizes of 256 and 512 with no overlap and different window functions. For $N = 1024$ this setting gives average over 2 or 4 spectral estimates. In the second method, parametric ARX modeling, a set of parametric multiple-input single output (MISO) ARX models

$$[y(t)]_i = \sum_{l=1}^{n_{\rm ARX}} a_{i,l} y_i(t-l) + \sum_{l=0}^{n_{\rm ARX}} B_{i,l} u(t-l) \quad \text{for } i = 1, 2, \dots p \tag{18}$$

are employed where $n_{\rm ARX}$ is the ARX model order. In the tests we evaluate the performance for all values of $n_{\rm ARX}$ from 1 to 30. The parameters are estimated from the $N = 1024$ time domain samples in the data window by solving a least-squares problem, see e.g. Ljung (1999). The frequency function estimate is given by

$$[\hat{G}_{\rm ARX}(\omega_q)]_{i,:} = \frac{\sum_{l=0}^{n_{\rm ARX}} \hat{B}_{i,l} e^{-j\omega_q l}}{1 + \sum_{l=1}^{n_{\rm ARX}} \hat{a}_{i,l} e^{-j\omega_q l}} \tag{19}$$

where $\hat{B}_{i,l}$ and $\hat{a}_{i,l}$ are the estimates of the ARX model parameters. The LRM, ARX and ETFE frequency function estimates are evaluated at the same set $\mathcal{Q}$ of frequencies.

The relative time elapsed to calculate the frequency function estimates is about five times slower for LRM and ARX as compared to the ETFE method. All methods are implemented in the Python language.

### *3.3 Results: vehicle model simulation data*

The three different methods, with varying hyperparameters, are evaluated on the data described in Section 3.1. For each method and hyperparameter setting the performance measured by *AUC* is established. The results are presented in Table 3, Table 2 and Table 4. For the LRM results in Table 3 we use the notation LRM:$n_{\rm LRM}$:$N_w$ to denote the specific choice of the hyperparameters local window size $N_w$ and local model order $n_{\rm LRM}$. For the ARX results we denote by ARX:$n_{\rm ARX}$ the results for the ARX model order $n_{\rm ARX}$. In each of the three tables the largest *AUC* value is in bold-face. We notice that LRM has the overasll largest value (98.0%) followed by ARX 97.2% and ETFE with 95.0%. We also notice that LRM seems to more robust with respect to the choice of hyperparameters compared to the other methods as the AUC is consistently larger than 94% except for the LRM:7:88 hyper-parameter setting.

### *3.4 Discussion*

The numerical results indicate that for the scenario analyzed all methods give some reasonable performance at least for some of the choices of the hyperparameters. For applications where the baseline model is unknown and must be estimated from data requires a non-trivial choice of model structure and hyperparameters. Methods which are robust to such choices can then be seen as a good method. The numerical results hence point to that LRM can be good choice for this type of application.

Table 2. *AUC* values for the ARX method. ARX:$n_{\rm ARX}$ denote denote results for ARX with model order $n_{\rm ARX}$

| | | | | | |
|---|---|---|---|---|---|
| ARX:2 | 83.8 | ARX:12 | 94.2 | ARX:22 | 91.6 |
| ARX:3 | 81.9 | ARX:13 | 93.6 | ARX:23 | 91.8 |
| ARX:4 | 91.9 | ARX:14 | 93.6 | ARX:24 | 91.2 |
| ARX:5 | 85.9 | ARX:15 | 93.7 | ARX:25 | 91.9 |
| ARX:6 | 94.9 | ARX:16 | 93.6 | ARX:26 | 91.7 |
| ARX:7 | 94.9 | ARX:17 | 93.3 | ARX:27 | 91.7 |
| ARX:8 | 96.0 | ARX:18 | 92.9 | ARX:28 | 91.2 |
| ARX:9 | **97.2** | ARX:19 | 92.5 | ARX:29 | 91.1 |
| ARX:10 | 93.8 | ARX:20 | 92.1 | ARX:30 | 90.8 |

Table 3. *AUC* values for the LRM method. LRM:$n_{\rm LRM}$:$N_w$ denote denote results for LRM with local model order $n_{\rm LRM}$ and local window size $N_w$

| | | | | | |
|---|---|---|---|---|---|
| LRM:2:14 | 94.5 | LRM:4:26 | 96.1 | LRM:6:38 | 96.5 |
| LRM:2:28 | 96.9 | LRM:4:52 | 96.0 | LRM:6:76 | 96.9 |
| LRM:3:20 | 95.7 | LRM:5:32 | 96.5 | LRM:7:44 | **98.0** |
| LRM:3:40 | 96.9 | LRM:5:50 | 97.2 | LRM:7:88 | 82.8 |

Table 4. *AUC* for the ETFE method for varying local window size and window functions

| Local window size | 256 | 512 |
|---|---|---|
| Rectangular | 94.7 | 88.1 |
| Hann | **95.0** | 89.6 |
| flattop | 91.9 | 85.8 |
| Kaiser ($\beta = 14$) | 94.2 | 87.8 |

## Appendix A. DISTRIBUTION OF THE TEST STATISTIC

*Lemma 1.* Assume the variables $x', x_1, \dots, x_N$ are i.i.d. from $\mathcal{CN}(\mu, \sigma^2)$ and let

$$\hat{\mu} = \frac{1}{N}\sum_{i=1}^{N} x_i, \quad \hat{\sigma}^2 = \frac{1}{N-1}\sum_{k=1}^{N} |x_i - \hat{\mu}|^2 \tag{A.1}$$

Then the test statistic

$$t = \frac{N|x' - \hat{\mu}|^2}{(N+1)\hat{\sigma}^2} \tag{A.2}$$

has a $F(2, 2N-2)$ distribution.

*Proof:* First we note that if $z \sim \mathcal{CN}(0, \sigma^2)$ then the real and imaginary part of $z$ are i.i.d. $\mathcal{N}(0, \sigma^2/2)$, a normal Gaussian distribution, Kay (1993). Clearly $(x' - \hat{\mu}) \sim \mathcal{CN}(0, \frac{N+1}{N}\sigma^2)$ and hence

$$t_1 = \frac{2N|x' - \hat{\mu}|^2}{\sigma^2(N+1)} \sim \chi^2_2 \tag{A.3}$$

has chi-squared distribution with 2 degrees of freedom (since the magnitude squared is the sum of the squared real and imaginary parts). From (A.1) we see that $\hat{\sigma}^2$ can be interpreted as the sum of the sample variance estimate of the real and imaginary parts respectively. Since the sample covariance based on $N$ samples from a Gaussian distribution has $N-1$ degrees of freedom, the sample covariance based on $N$ samples from a complex Gaussian distribution will have $2N-2$ degrees of freedom and we conclude that the statistic

$$t_2 = \frac{2N-2}{\sigma^2}\hat{\sigma}^2 \sim \chi^2_{2N-2} \tag{A.4}$$

i.e. a chi-squared distribution of $2N-2$ degrees of freedom. Since sample mean and sample covariance are independent

for the Gaussian case this property is carried over to the complex Gaussian case and hence it follows that $t_1$ and $t_2$ are independent since $(x' - \hat{\mu})$ is independent of $\hat{\sigma}^2$. The result now follows since $t = \frac{t_1/2}{t_2/(2N-2)}$. See e.g. Grimmett and Stirzaker (2001) for details of the $F$-distribution. ■

*Lemma 2.* Assume the variables $t_1, \ldots, t_n$ are i.i.d. from $F(2a, 2b)$, $a, b > 0$. Then

$$T' = \frac{a}{b} \sum_{i=1}^{n} t_i \tag{A.5}$$

is distributed according to the Beta prime distribution denoted by $\beta'(\gamma, \delta)$ and

$$T = \frac{a\delta}{b\gamma} \sum_{i=1}^{n} t_i \tag{A.6}$$

is distributed according to $F(2\gamma, 2\delta)$ with parameters

$$\begin{aligned} \gamma &= \frac{an(a(b-2)n + a + (b-1)^2)}{(b-1)(a+b-1)} \\ \delta &= \frac{a((b-2)n+2) + (b-1)b}{a+b-1} \end{aligned} \tag{A.7}$$

*Proof:* It is well known that if $t_i$ has an $F(2a, 2b)$ distribution then its equivalent to $\frac{a}{b} t_i \sim \beta'(a, b)$. Furthermore, the Beta prime distribution is infinitely divisible; specifically, this means that a sum of $n$ i.i.d. Beta prime distributions is also Beta prime distributed. The parameters $\gamma$ and $\delta$ are found by matching the first two moments. See e.g. Steutel and van Harn (2003) p.415 and 508 for more information. Since $T' \sim \beta'(\gamma, \delta)$ we can use the above result and get that $T = \frac{\gamma}{\delta} T' \sim F(2\gamma, 2\delta)$, where we use that $a, b > 0$ implies that $\gamma, \delta > 0$. ■

*Theorem 1.* Let $c = \frac{\delta N_B}{\gamma(N_B^2 - 1)}$ in (15). Then the test statistic $T$ in (15) has an $F(\gamma, \delta)$ distribution. With $n = Qmp$, $a = 1$ and $b = N_B - 1$, $\gamma$ and $\delta$ are given by (A.7).

*Proof:* The test statistic $T$ can be reformulated as

$$\begin{aligned} T &= c \sum_{q=1}^{Q} (\operatorname{vec} \tilde{G}_q - \operatorname{vec} \hat{G}_q)^* \hat{R}_q^{-1} (\operatorname{vec} \tilde{G}_q - \operatorname{vec} \hat{G}_q) \\ &= c \sum_{i=1}^{N_T} \frac{|x_i - \hat{\mu}_i|^2}{\hat{\sigma}_i^2} \end{aligned} \tag{A.8}$$

where $N_T = Qmp$, $x_i \sim \mathcal{CN}(\mu_i, \sigma_i^2)$ and $\hat{\mu}_i$ and $\hat{\sigma}_i^2$ are the sample mean and sample covariance estimates based on $N_B$ i.i.d. samples from $\mathcal{CN}(\mu_i, \sigma_i^2)$ according to the formulation of Lemma 1. The result of Lemma 1 show that

$$T = c' \frac{N_B}{N_B + 1} \sum_{i=1}^{N_T} \frac{|x_i - \hat{\mu}_i|^2}{\hat{\sigma}_i^2} \tag{A.9}$$

$T/c'$ is hence a sum of $N_T$ i.i.d. random variables with an $F(2, 2N_B - 2)$ distribution. Finally by setting $c' = \frac{a\delta}{b\gamma}$, $n = N_T = Kmp$, $a = 1$ and $b = N_B - 1$ the result follows by Lemma 2. ■

## REFERENCES


Basseville, M., Mevel, L., and Goursat, M. (2004). Statistical model-based damage detection and localization: subspace-based residuals and damage-to-noise sensitivity ratios. *Journal of Sound and Vibration*, 275(3), 769 – 794.

Basseville, M. and Nikiforov, I.V. (1993). *Detection of Abrupt Changes: Theory and Application*. Prentice-Hall.

Doebling, S.W., Farrar, C.R., Prime, M.B., and Shevitz, D.W. (1996). Damage identification and health monitoring of structural and mechanical systems from changes in their vibration characteristics: a literature review. Technical report, Los Alamos National Lab., NM (United States).

Grimmett, G. and Stirzaker, D. (2001). *Probability and random processes*. Oxford University Press, Oxford, 3rd edition.

Hastie, T., Tibshirani, R., and Friedman, J. (2009). *The Elements of Statistical Learning: Data Mining, Inference, and Prediction.* Springer, 2nd edition.

Johnson, T.J. and Adams, D.E. (2002). Transmissibility as a Differential Indicator of Structural Damage. *Journal of Vibration and Acoustics*, 124(4), 634–641. doi: 10.1115/1.1500744.

Kailath, T. (1980). *Linear Systems*. Prentice-Hall, Englewood Cliffs, New Jersey.

Kay, S.M. (1993). *Fundamentals of Statistical Signal Processin - Estimation Theory*. Prentice Hall.

Kopsaftopoulos, F.P. and Fassois, S.D. (2010). Vibration based health monitoring for a lightweight truss structure: Experimental assessment of several statistical time series methods. *Mechanical Systems and Signal Processing*, 24(7), 1977–1997.

Ljung, L. (1999). *System Identification: Theory for the User*. Prentice-Hall, Englewood Cliffs, New Jersey, second edition.

McKelvey, T. (2000). On the Finite Length DFT of Input-Output Signals of Multivariable Linear Systems. In *Proc.of 39th Conference on Decision and Control*, volume 5, 5190–5191. Sydney, Australia.

McKelvey, T. and Guerin, G. (2012). Non-parametric frequency response estimation using a local rational model. In *Proc. 16th IFAC Symposium on System Identification*. IFAC, Brussels, Belgium.

Steutel, F.W. and van Harn, K. (2003). *Infinite Divisibility of Probability Distributions on the Real Line*. CRC Press. doi:10.1201/9780203014127.

Voorhoeve, R., van der Maas, A., and Oomen, T. (2018). Non-parametric identification of multivariable systems: A local rational modeling approach with application to a vibration isolation benchmark. *Mechanical Systems and Signal Processing*, 105, 129–152. doi: 10.1016/j.ymssp.2017.11.044.

Yin, S., Ding, S.X., Xie, X., and Luo, H. (2014). A review on basic data-driven approaches for industrial process monitoring. *IEEE Transactions on Industrial Electronics*, 61(11), 6418–6428. doi:10.1109/TIE.2014.2301773. URL `https://ieeexplore.ieee.org/document/6717991`.